AMERICAN SOCIETY FOR MICROBIOLOGY | mBio®

RESEARCH ARTICLE

Candida albicans-Induced Epithelial Damage Mediates Translocation through Intestinal Barriers

Stefanie Allert,[a] Toni M. Förster,[a] Carl-Magnus Svensson,[b] Jonathan P. Richardson,[c] Tony Pawlik,[d] Betty Hebecker,[a,d,e] Sven Rudolphi,[d] Marc Juraschitz,[a] Martin Schaller,[f] Mariana Blagojevic,[c] Joachim Morschhäuser,[g] Marc Thilo Figge,[b,h] Ilse D. Jacobsen,[d,i] Julian R. Naglik,[c] Lydia Kasper,[a] Selene Mogavero,[a] Bernhard Hube[a,i]

[a]Department of Microbial Pathogenicity Mechanisms, Hans-Knöll-Institute, Jena, Germany
[b]Research Group Applied Systems Biology, Hans-Knöll-Institute, Jena, Germany
[c]Mucosal & Salivary Biology Division, Dental Institute, King's College London, London, United Kingdom
[d]Research Group Microbial Immunology, Hans-Knöll-Institute, Jena, Germany
[e]Aberdeen Fungal Group, MRC Centre for Medical Mycology, University of Aberdeen, Aberdeen, United Kingdom
[f]Department of Dermatology, University Hospital Tübingen, Tübingen, Germany
[g]Institute for Molecular Infection Biology, University of Würzburg, Würzburg, Germany
[h]Faculty of Biological Sciences, Friedrich-Schiller-University Jena, Jena, Germany
[i]Institute of Microbiology, Friedrich-Schiller-University Jena, Jena, Germany

ABSTRACT Life-threatening systemic infections often occur due to the translocation of pathogens across the gut barrier and into the bloodstream. While the microbial and host mechanisms permitting bacterial gut translocation are well characterized, these mechanisms are still unclear for fungal pathogens such as *Candida albicans*, a leading cause of nosocomial fungal bloodstream infections. In this study, we dissected the cellular mechanisms of translocation of *C. albicans* across intestinal epithelia *in vitro* and identified fungal genes associated with this process. We show that fungal translocation is a dynamic process initiated by invasion and followed by cellular damage and loss of epithelial integrity. A screen of >2,000 *C. albicans* deletion mutants identified genes required for cellular damage of and translocation across enterocytes. Correlation analysis suggests that hypha formation, barrier damage above a minimum threshold level, and a decreased epithelial integrity are required for efficient fungal translocation. Translocation occurs predominantly via a transcellular route, which is associated with fungus-induced necrotic epithelial damage, but not apoptotic cell death. The cytolytic peptide toxin of *C. albicans*, candidalysin, was found to be essential for damage of enterocytes and was a key factor in subsequent fungal translocation, suggesting that transcellular translocation of *C. albicans* through intestinal layers is mediated by candidalysin. However, fungal invasion and low-level translocation can also occur via non-transcellular routes in a candidalysin-independent manner. This is the first study showing translocation of a human-pathogenic fungus across the intestinal barrier being mediated by a peptide toxin.

IMPORTANCE *Candida albicans*, usually a harmless fungus colonizing human mucosae, can cause lethal bloodstream infections when it manages to translocate across the intestinal epithelium. This can result from antibiotic treatment, immune dysfunction, or intestinal damage (e.g., during surgery). However, fungal processes may also contribute. In this study, we investigated the translocation process of *C. albicans* using *in vitro* cell culture models. Translocation occurs as a stepwise process starting with invasion, followed by epithelial damage and loss of epithelial integrity. The ability to secrete candidalysin, a peptide toxin deriving from the hyphal protein

Received 2 May 2018 **Accepted** 3 May 2018 **Published** 5 June 2018

Citation Allert S, Förster TM, Svensson C-M, Richardson JP, Pawlik T, Hebecker B, Rudolphi S, Juraschitz M, Schaller M, Blagojevic M, Morschhäuser J, Figge MT, Jacobsen ID, Naglik JR, Kasper L, Mogavero S, Hube B. 2018. *Candida albicans*-induced epithelial damage mediates translocation through intestinal barriers. mBio 9:e00915-18. https://doi.org/10.1128/mBio.00915-18.

Editor James W. Kronstad, University of British Columbia

Address correspondence to Bernhard Hube, bernhard.hube@leibniz-hki.de.

S.A. and T.M.F. contributed equally to this work.

This article is a direct contribution from a Fellow of the American Academy of Microbiology. Solicited external reviewers: Elaine Bignell, University of Manchester; Michael Lorenz, University of Texas Health Science Center.

Ece1, is key: *C. albicans* hyphae, secreting candidalysin, take advantage of a necrotic weakened epithelium to translocate through the intestinal layer.

KEYWORDS *Candida albicans*, candidalysin, host cell damage, host cell invasion, intestinal barrier, necrosis, translocation

Candida albicans is one of the predominant fungal species that colonizes the mucosal surfaces of most humans as a harmless member of the normal microbiota (1, 2). However, under certain circumstances, *C. albicans* can become pathogenic and cause diseases ranging from common superficial to severe systemic infections (3, 4). These life-threatening disseminated infections are initiated by endogenous colonizers, which translocate from mucosal surfaces into the bloodstream. Several studies have demonstrated that the intestinal population of *C. albicans* is the main source of disseminated candidiasis (5–11). However, in a healthy host, the intestinal epithelium, together with mucosal immune cells, constitute a stable barrier preventing *C. albicans* from translocating into the bloodstream. Host defense against translocation is further augmented by the physical barrier functions of the epithelial layer, with tight junctions and adherens junctions sealing paracellular spaces (12), and a mucous layer that protects the epithelium, thereby directly affecting *C. albicans* physiology and morphology (13). In addition, a balanced and diverse microbiota (14), the secretion of antimicrobial peptides (AMPs) (15), and the concerted activity of the innate and adaptive immune systems (14, 16) act to reduce hyphal burdens during periods of fungal overgrowth and restrict the fungus to the commensal (yeast) morphology. However, dysfunctions in these protective mechanisms can favor *C. albicans* translocation.

Predisposing conditions that trigger the commensal-to-pathogen shift and translocation of *C. albicans* are often iatrogenic. These conditions include an imbalance of the resident microbiota by use of antibiotics, a compromised immune system (e.g., due to chemotherapy or immunosuppressive therapy), or damage of epithelial barrier functions by iatrogenic impairment, for instance due to cytostatic treatment, surgery, or trauma (17, 18). Consequently, disseminated candidiasis is typically a nosocomial infection, and intensive care unit (ICU) patients are particularly susceptible to invasive *C. albicans* infections (19–21).

In principle, initiation of disseminated candidiasis requires at least one of four events: (i) entry of *C. albicans* cells by direct invasion of epithelial cells (ECs) from intestinal mucosal surfaces into blood capillaries or vessels; (ii) indirect translocation of *C. albicans* cells phagocytosed by host immune cells ("sampling"); (iii) direct damage of mucosal barriers, for example due to surgery, polytrauma, or drug treatment; or (iv) spread from fungal biofilms established on medical devices such as catheters (22, 23).

Translocation of *C. albicans* in murine models requires a combination of increased fungal colonization via removal of the bacterial microbiota, neutropenia, and intestinal barrier dysfunction in order to establish disseminated disease (24). Importantly, infrequent fungal translocation may also occur without epithelial damage under conditions of enhanced fungal colonization following antibiotic pretreatment (23), and it does not always result in systemic disease in immunocompetent mice (25).

Although dissemination of *C. albicans* from the intestinal tract has been studied *in vivo* (5, 24–27), the molecular mechanism of *C. albicans* translocation across intestinal barriers via epithelial invasion and the fungal attributes required for this process are poorly characterized. Pathogenic interactions of *C. albicans* with ECs can be divided into three stages: adhesion, invasion, and damage (28–31). Each of these steps requires hypha formation and the expression of hypha-associated genes. For example, hypha-associated expression of *ALS3* permits not only adhesion (32) but also induced endocytosis (33) and iron acquisition (34). Expression of *ECE1* (encoding the peptide toxin candidalysin) is essential for epithelial damage (35) and is the missing link between hypha formation and host cell damage (36).

In this study, we used an *in vitro* translocation model to characterize the events associated with *C. albicans* translocation through an intact intestinal barrier. We show

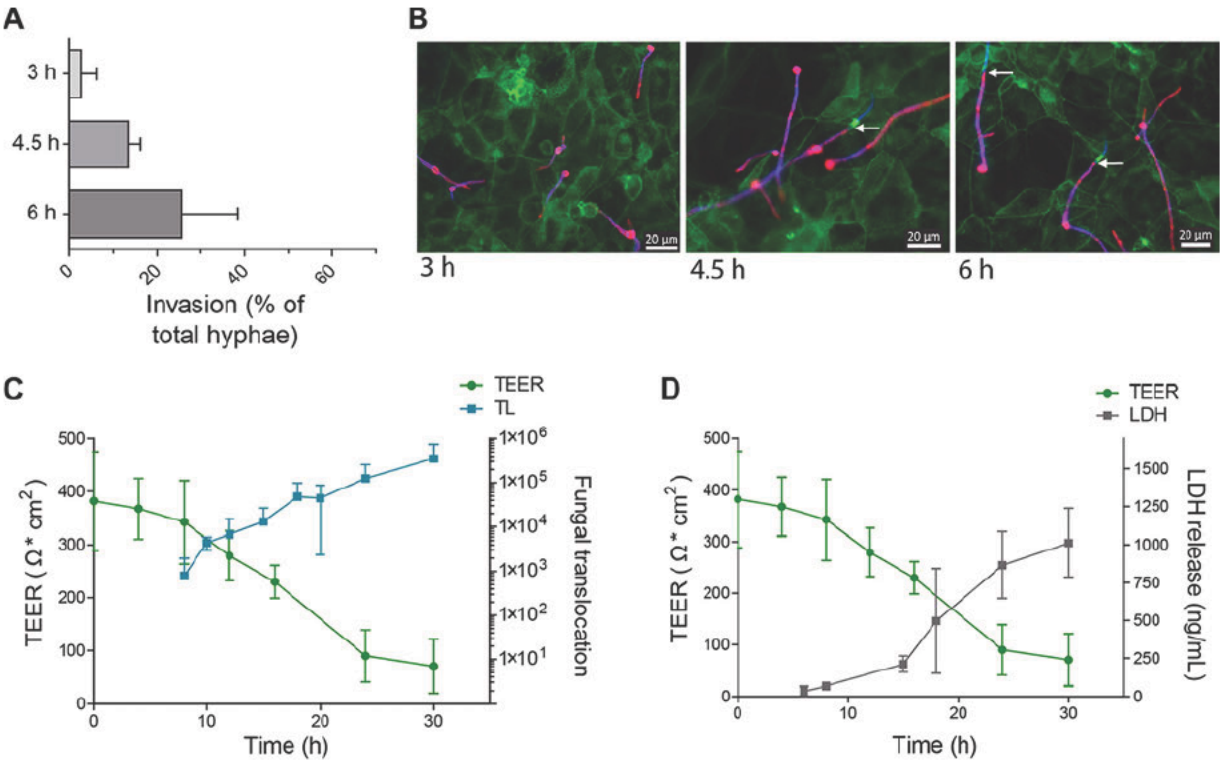

FIG 1 Infection of C2BBe1 IECs with wild-type *C. albicans*. (A) Invasion of *C. albicans* into C2BBe1 cells at 3 h, 4.5 h, and 6 h p.i. was quantified by differential fluorescence microscopy staining. The percentage of invasive hyphae relative to total *C. albicans* visible hyphae is shown. (B) Representative fluorescence microscopy images of differential staining to quantify *C. albicans* invasion. Extracellular *C. albicans* (pink), *C. albicans* (blue), and actin (green) are indicated. The white arrows indicate the entry point of the invading hypha. (C) Quantification of C2BBe1 barrier integrity as measured by TEER, and fungal translocation (number of translocated cells) after infection with *C. albicans* SC5314. (D) Release of LDH from C2BBe1 cells after infection with *C. albicans* SC5314. Data are presented as means ± standard deviations (SD) (error bars) from at least three independent experiments.

that translocation in this model mainly occurs via a transcellular route associated with fungus-induced necrotic, but not apoptotic, cell death. A screen of >2,000 *C. albicans* gene deletion mutants identified several genes associated with intestinal epithelial damage. Selected damage-defective mutants were analyzed for their impact on epithelial barrier function and translocation. Our data suggest that *C. albicans* transcellular translocation through intestinal layers requires candidalysin-induced epithelial damage. This is the first study that shows a peptide toxin-mediated translocation of a human-pathogenic fungus.

RESULTS

Dynamics of fungal invasion, epithelial damage, and loss of epithelial barrier integrity during translocation of *Candida albicans* through intestinal epithelial layers. A combination of predisposing factors, including damage to epithelial barriers acquired during surgery or polytrauma, contribute to disseminated candidiasis. However, translocation of *C. albicans* across epithelial barriers can also occur without iatrogenic or accidental epithelial damage. We hypothesized that this particular type of translocation from the gut into the bloodstream requires invasion into intestinal epithelial cells (IECs) that is associated with fungus-induced cellular damage and loss of epithelial barrier integrity. To investigate the dynamics of this process, we established a translocation assay using the C2BBe1 cell line, a subclone of the human intestinal cell line Caco-2 (37), in a transwell system, by modifying previous protocols (29, 38, 39). We infected C2BBe1 enterocytes with wild-type (WT) *C. albicans* and monitored fungal invasion (via differential staining), host cell damage (via release of epithelial lactate dehydrogenase [LDH]), loss of epithelial monolayer integrity (via quantification of TEER [transepithelial electrical resistance]), and translocation (via fungal burdens) (Fig. 1).

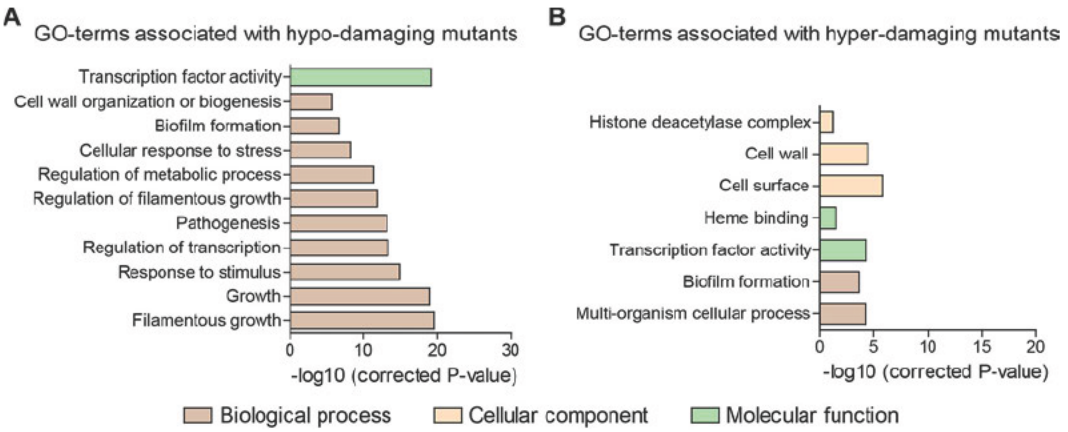

FIG 2 Gene Ontology (GO) term analysis of hypo- and hyperdamaging mutants. Gene deletions associated with significantly decreased (A) or increased (B) damage.

Low-level invasion (3.6%) of *C. albicans* into C2BBe1 cells was observed 3 h postinfection (p.i.) and steadily increased over time (Fig. 1A and B). The observed invasion did not correlate with a loss of epithelial barrier integrity, epithelial damage, or translocation during the early stages (<3 h) of infection (Fig. 1C and D). However, extensive epithelial damage, loss of barrier integrity, and translocation were observed between 8 h and 30 h p.i. (Fig. 1C and D).

Previous studies have shown that invasion of *C. albicans* into differentiated enterocytes (Caco-2) is a hypha-dependent, fungus-driven process that occurs via active penetration, but not induced endocytosis, in contrast to other epithelial cells such as oral ECs (29, 40). To investigate whether the same was also true for the invasion of *C. albicans* into the C2BBe1 subclone, differentiated C2BBe1 cells were treated with the actin polymerization inhibitor cytochalasin D, which blocks induced endocytosis. Cytochalasin D did not impair invasion of *C. albicans* into C2BBe1 cells, and UV-killed hyphae, which are endocytosed by oral ECs (29), were not endocytosed by C2BBe1 cells (see Fig. S1 in the supplemental material). Therefore, invasion into differentiated C2BBe1 intestinal cells is a fungus-driven process.

Large-scale screening of *C. albicans* mutant libraries identifies genes important for epithelial damage. Since *in vitro* translocation of *C. albicans* correlated with cytotoxicity, we investigated whether *C. albicans* factors necessary for damage of IECs might also play a role in fungal translocation. Therefore, we screened three *C. albicans* gene deletion mutant libraries (41–43) for their ability to damage Caco-2 IECs by quantifying LDH levels. A total of 2,034 *C. albicans* gene deletion mutants were screened, including 1,165 homozygous open reading frame (ORF) deletions (approximately 20% of all annotated *C. albicans* genes [Data Set S1]). These included genes required for a broad spectrum of biological processes and potential virulence-associated traits (41), including transcriptional regulators (43). In total, we identified 172 *C. albicans* gene deletion mutants that caused significantly less damage ($<\mu - 2\sigma$) compared to their respective WT control (shown in red in Data Set S1 in the supplemental material; see Data Set S2 also). *In silico* Gene Ontology (GO) term analysis revealed that these genes are putatively involved in filamentation, pathogenesis, and stress responses (among other functions) (Fig. 2A). The *Candida* Genome Database (44) identified 67 of these genes as having unknown function (shown in blue in Data Set S2). We also identified 102 *C. albicans* gene deletion mutants that caused more damage ($>\mu + 2\sigma$) to Caco-2 IECs compared to the WT (shown in green in Data Set S1; see Data Set S2 also). *In silico* analysis of the corresponding genes of this subgroup showed putative associations with biofilm formation and cell surface composition (among other functions) (Fig. 2B). Fifty-two of these genes encode proteins with unknown function (shown in blue in Data Set S2).

The cytotoxicity analysis was performed in parallel with general growth assays in YPD broth (see Materials and Methods) and morphology analysis on IECs (Data Set S2). *C. albicans* gene deletion mutants with a general growth defect in complete medium and mutants with severe morphological defects were excluded from further analysis, since such phenotypes were expected to lead to unspecific or morphology-related reductions in damage. Indeed, the majority of gene deletion mutants that were compromised for hypha formation were also severely attenuated in their ability to cause damage (Data Set S2). Of the 172 gene deletion mutants identified that were hypodamaging to Caco-2 IECs, 38 mutants with no obvious growth or filamentation defects were selected for further analysis in epithelial damage assays using differentiated C2BBe1 cells (shown in orange in Data Set S2).

On the basis of these data, nine genes were selected for further analysis: *PRN4*, orf19.2797, *NPR2*, *AAF1*, *HMA1*, *TEA1*, orf19.3335, *PEP12*, and *ECE1* (Table S1). Selection criteria included (i) previously uncharacterized genes (*PRN4*, *NPR2*, orf19.2797, *HMA1*, *TEA1*, and orf19.3335), (ii) genes uncharacterized for interaction with IECs (*AAF1*, *PEP12*, and *ECE1*) (35, 45–47), and/or (iii) genes with putative functions, including urea transport, transcriptional regulation, ligand binding, and cytolytic toxicity (Table S2).

Since it is frequently observed that the altered phenotypes of mutants identified in the screen were not due to targeted gene deletion, but rather unspecific genomic alterations, and to exclude differences between genetic backgrounds, all nine selected mutants were recreated in a *C. albicans* BWP17 genetic background (48). These mutants were characterized in more detail (below), including quantification of their hyphal length, adhesion, invasion potential, and damage (Fig. 3 and S2). All mutants were significantly impaired in their ability to cause damage to differentiated C2BBe1 cells 24 h p.i., quantified by LDH measurements (Fig. 3A), with the exception of the *prn4*Δ/Δ mutant, which exhibited WT levels of damage and was thus not further investigated. The degree of damage reduction varied from moderate (less than 50%; *npr2*Δ/Δ, orf19.2797Δ/Δ, *aaf1*Δ/Δ, and *hma1*Δ/Δ) to severe (more than 50%: *tea1*Δ/Δ, orf19.3335Δ/Δ, *pep12*Δ/Δ, and *ece1*Δ/Δ). Interestingly, almost every mutant showed a unique pattern of phenotypic defects potentially responsible for the reduced damage observed (Fig. 3). For example, invasion of IECs by the *aaf1*Δ/Δ and *pep12*Δ/Δ mutants was significantly reduced, the *pep12*Δ/Δ mutant had significantly shorter hyphae compared to the WT hyphae, while the *hma1*Δ/Δ and orf19.3335Δ/Δ mutants showed moderately reduced adhesion, invasion, and hyphal length. In contrast, the *ece1*Δ/Δ mutant did not show any obvious phenotypic alteration except reduced damage (Fig. 3C and D; Fig. S2).

Translocation of *C. albicans* through enterocytes is associated with damage and loss of epithelial barrier integrity. Our initial experiments demonstrate that translocation of *C. albicans* through the intestinal layer is associated with cellular damage and loss of epithelial integrity (Fig. 1). Accordingly, we tested whether decreased levels of epithelial damage were associated with a lower level of epithelial translocation. Further, we compared the ability of a "normal"-damaging mutant (*bas1*Δ/Δ) and a hyperdamaging mutant (*snt1*Δ/Δ; shown in green in Data Set S1; see Data Set S2 also) to translocate across an epithelial barrier. Several well-characterized control strains were included in this analysis, including mutants lacking genes involved in hyphal morphogenesis, hyphal maintenance, biofilm formation, adhesion, protein processing, or secreted protease activity (Table S2). Furthermore, translocation through a blank insert in the absence of an EC layer was quantified to exclude translocation impairment independent of host cells (see Materials and Methods; Fig. S3A).

Figure 4 summarizes the epithelial damage, fungal translocation, and epithelial integrity data for all 19 mutants. To identify correlations between mutant phenotypes and the ability to translocate through epithelial layers, and thus to identify properties associated with *C. albicans* translocation, we used a bioinformatic approach. First, we applied a density-based spatial clustering with noise (DBSCAN) algorithm (49) to categorize *C. albicans* mutants into groups with similar behavior based on the three parameters "epithelial damage," "epithelial integrity," and "fungal translocation" (Fig. 4

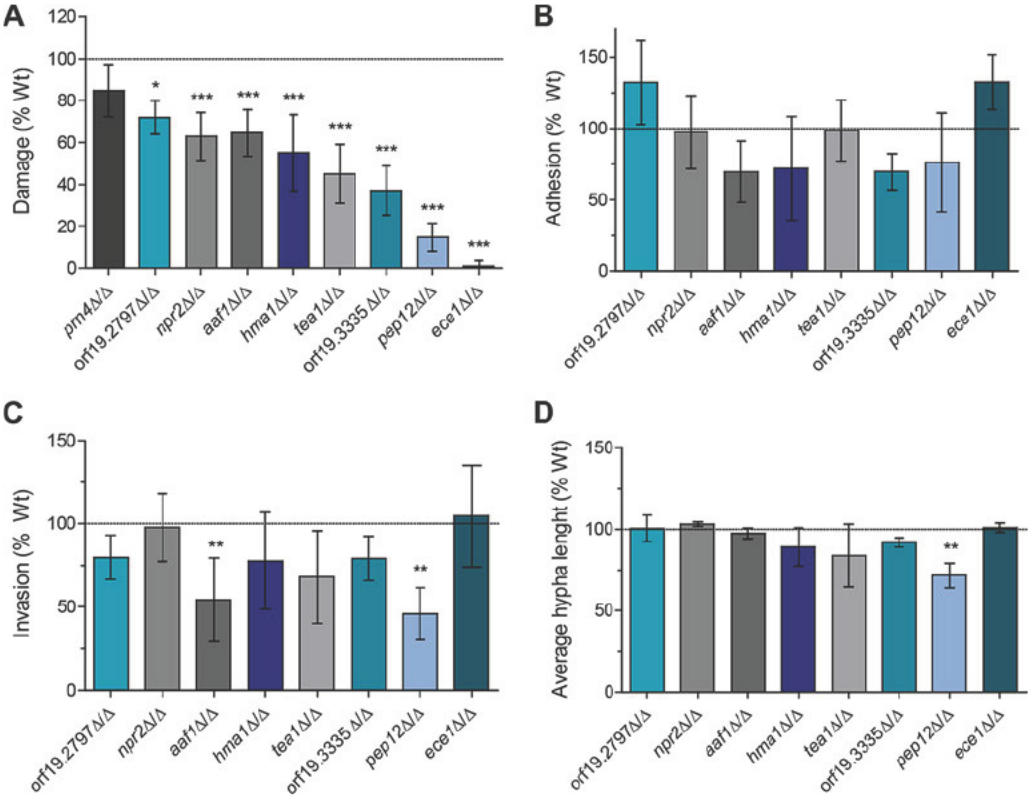

FIG 3 *In vitro* characterization of selected *C. albicans* mutants on C2BBe1 IECs. (A) C2BBe1 IECs were infected with selected *C. albicans* mutants, and cellular damage 24 h p.i. was quantified by LDH assay. The mean cellular damage induced by wild-type *C. albicans* was 865 ± 219 ng/ml LDH (dotted line). (B) The adhesion of selected *C. albicans* mutant strains to C2BBe1 IECs 1 h p.i. was quantified as described in Materials and Methods. The mean adhesion of WT *C. albicans* to C2BBe1 cells was 9.2% ± 5.7% (dotted line). (C) The invasion of selected *C. albicans* mutant strains into C2BBe1 IECs 5 h p.i. was quantified as described in Materials and Methods. The mean invasion level of WT *C. albicans* was 12.3% ± 5.9% (dotted line). (D) C2BBe1 IECs were infected with selected *C. albicans* mutants, and their mean hyphal length 5 h p.i. was determined. The mean length of WT *C. albicans* hyphae was 77.8 ± 12.6 μm (dotted line). All values are presented as mean ± SD relative to the WT. Values that are statistically significantly different are indicated by asterisks as follows: *, $P \leq 0.05$; **, $P \leq 0.01$; ***, $P \leq 0.001$.

and S4). This led to the arrangement of strains in three clusters: (i) cluster I strains showing low damage, low translocation rates, and almost unaltered TEER values; (ii) cluster II strains being similar to the wild type; and (iii) cluster III strains displaying low damage and translocation, but wild-type-like loss of TEER. However, some *C. albicans* mutants could not be assigned to any cluster and were unique in their behavior in the translocation model. Interestingly, the *snt1*Δ/Δ mutant, a member of the hyperdamaging group, was significantly attenuated in causing loss of epithelial integrity and translocation through epithelial layers, whereas the hypha-deficient *hgc1*Δ/Δ mutant caused significantly reduced damage but could still translocate, while epithelial integrity was reduced by approximately 50%. An *ece1*Δ/Δ mutant displayed a moderate loss of epithelial integrity (50%) compared to the WT, but it caused almost no damage and exhibited a 75% reduction in translocation. Finally, the unassigned SAP mutants *sap1-3*Δ/Δ and *sap4-6*Δ/Δ showed a very strong similarity to cluster II, except for increased translocation potential, which was related to an altered ability to cross a blank transwell.

On the basis of these observations, a bioinformatic analysis was performed between pairings of the three parameters; "epithelial damage," "epithelial integrity," and "fungal translocation" to understand their reciprocal relationship. According to Pearson's correlation analysis, all three parameters were significantly correlated, while according to Spearman's correlation analysis, translocation and epithelial integrity (TEER) were not significantly correlated (Fig. 5). Both types of correlations were of moderate magni-

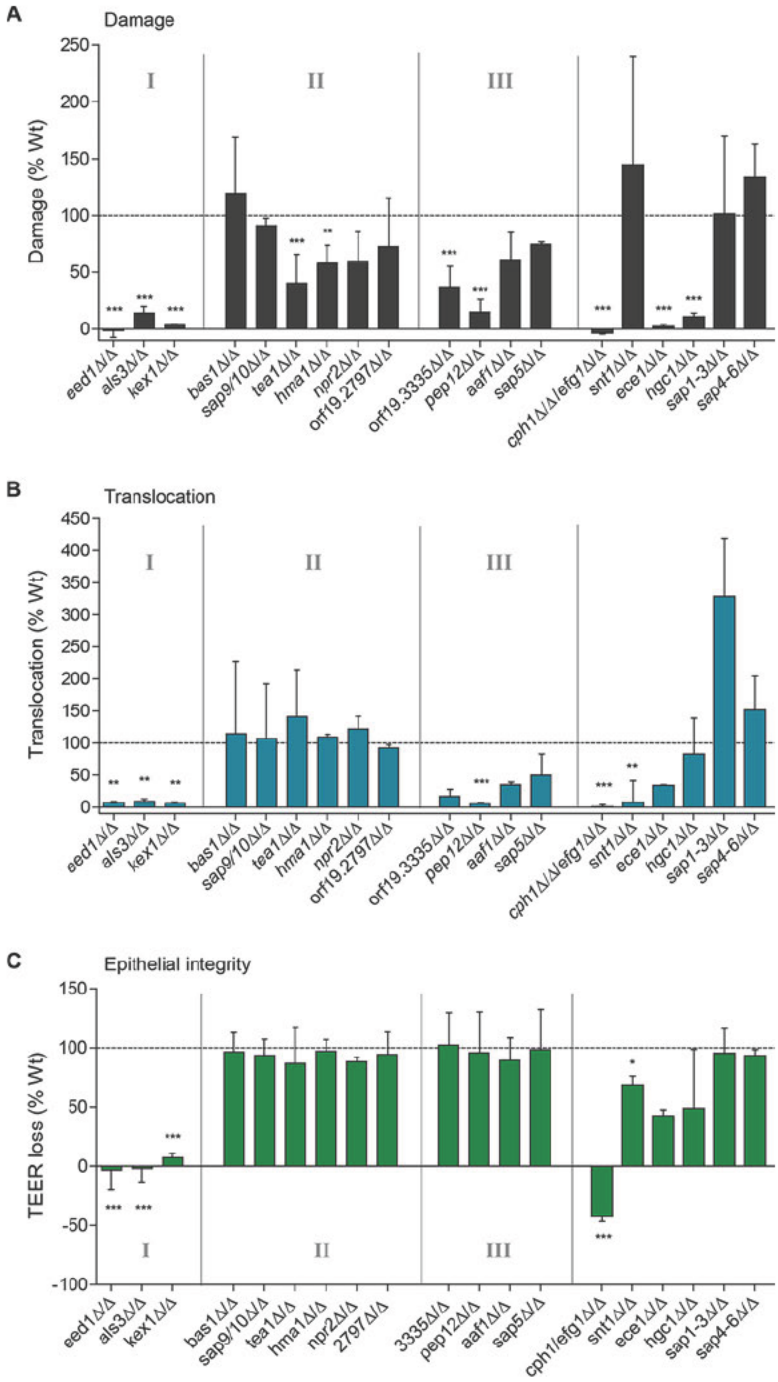

FIG 4 Characterization of damage, translocation, and loss of TEER by selected and control mutants. (A) *C. albicans* gene deletion mutants were analyzed for their ability to damage C2BBe1 IECs by LDH assay. (B) Translocation of *C. albicans* gene deletion mutants across a differentiated C2BBe1 intestinal epithelial barrier. (C) Assessment of C2BBe1 epithelial barrier integrity in response to *C. albicans* gene deletion mutants at 24 h p.i. as measured by loss of TEER. Data are expressed as TEER loss as a percentage of the wild-type *C. albicans*-infected cells. Strains are arranged in clusters (I to III) according to bioinformatic analysis. Cluster I exhibited low damage, translocation, and loss of TEER. Cluster II contains wild-type-like mutants. Cluster III exhibited low damage and translocation but wild-type-like loss of TEER. All values are presented as median plus range relative to the WT (dotted line). Statistical significance: *, $P \leq 0.05$; **, $P \leq 0.01$; ***, $P \leq 0.001$.

tude (~0.5, see Fig. 5B), which is explained by the strong variability among strains. For example, although translocation generally increases with increased epithelial damage (LDH), the *snt1*Δ/Δ mutant displays reduced translocation, even though it has the highest epithelial damage of all mutants. Next, to quantify any nonlinear behaviors in

A

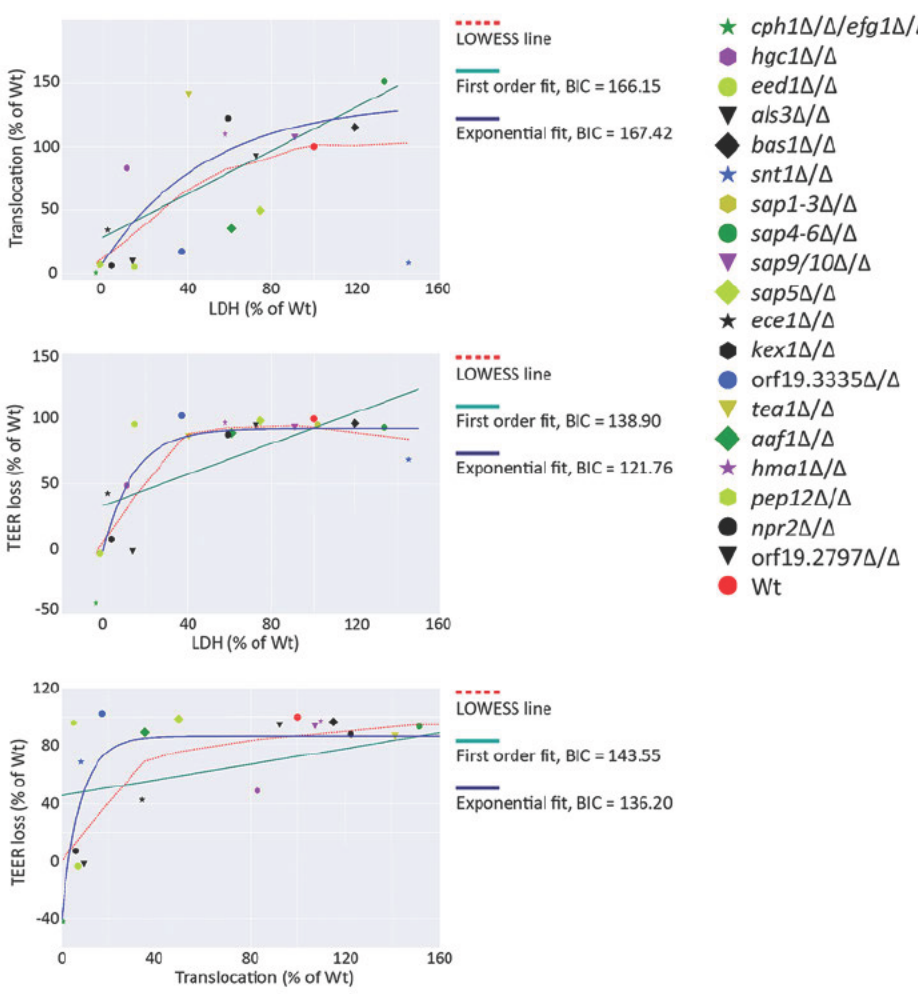

B

	LDH-Translocation	LDH-TEER	Translocation-TEER
Pearson's correlation coefficient	0.53 (p = 0.029)	0.64 (p = 0.003)	0.49 (p = 0.032)
Spearman's correlation coefficient	0.62 (p = 0.005)	0.58 (p = 0.009)	0.43 (p = 0.064)

FIG 5 Bioinformatic analysis of *C. albicans*-induced epithelial damage, loss of epithelial integrity, and fungal translocation. Data obtained from WT and mutant strains of *C. albicans* for damage (LDH release), change in epithelial integrity (TEER), and translocation (CFU) were analyzed. (A) Pairwise correlation analysis of epithelial damage (LDH), barrier integrity (TEER), and translocation (CFU). In addition to the median value for each strain, the fit of a first-order polynomial and an exponential fit is shown together with a LOWESS line that describes a parameter-free smoothing to visualize the overall trend. The Bayesian information criterion (BIC) of each fit is given. Note that the *sap1-3*Δ/Δ strain is not visible, since it has extremely high translocation values; this data point was, however, taken into account in the calculation of correlations and in the curve fitting. (B) Correlation coefficients of the pairwise measurements presented. The respective *P* values are calculated using a two-tailed Student's *t* test.

the correlations, we fitted a first-order polynomial and an exponential function of the form $y = Ae^{-\alpha x} + B$ to each pair of measurements and evaluated the most appropriate model using the Bayesian information criterion (BIC) (50). The choices of independent measures (x) and dependent measures (y) are picked according to the respective x- and y-axes in Fig. 5A. We plotted the fitted polynomials and the LOWESS line (51) (i.e., a nonparametric smoothing that visualizes overall trends in noisy data) and provided the BIC values in Fig. 5A.

For epithelial damage and translocation, there was no improvement in the BIC using the exponential fit compared to a first-order polynomial, and the latter was observed to be close to the LOWESS line. This indicated a close-to-linear relationship between

damage and translocation, suggesting that these two outcomes are most often the result of the same process or closely related processes. For epithelial damage and integrity, the LOWESS line and the exponential function tracked closely with another, which coincides with a considerable decrease in the BIC. This indicates that in the presence of epithelial damage, the epithelial integrity decreases rapidly to a minimum, independent of additional damage being induced. Last, translocation and epithelial integrity show the lowest correlation with a small improvement in BIC values using an exponential function. The increase is not as large as for epithelial damage and integrity, and the clear deviation from the LOWESS line indicates that neither function is able to track the structure of the data very well. The lack of significance in Spearman's correlation coefficient can be explained by the structure of the data as seen in Fig. 5A. For strains with high translocation (>90% of WT), the epithelial integrity is consistently low, i.e., around WT levels (100% TEER loss), while for low translocation values (0 to 40% of WT), there is no clear structure in the epithelial integrity data. Pearson's correlation coefficient takes into account that very high translocation indicates low epithelial integrity, while the nonsignificant Spearman's correlation coefficient captures the lack of correlations within strains with low and high translocation. This reveals that while decreased epithelial integrity is a prerequisite for translocation, this does not predict fungal translocation (i.e., as seen with *pep12*Δ/Δ [Fig. 4]).

Dissecting the potential routes of *C. albicans* translocation through enterocyte layers. Our data and bioinformatic analyses suggest that while epithelial damage and loss of epithelial integrity are associated with translocation of *C. albicans* through epithelial barriers, this does not always predict the amount of fungal translocation. These analyses suggest two basic routes of gut translocation by *C. albicans*: paracellular (between adjacent IECs) and transcellular (through viable or nonviable enterocytes from the apical side to the basolateral side) (Fig. 6A, routes I to III). The latter would potentially be associated with EC death, which could either be necrotic or apoptotic.

Next, we investigated the role of epithelial apoptosis versus necrosis for transcellular translocation (Fig. 6). The contribution of enterocyte apoptosis following *C. albicans* infection was monitored by annexin V staining and fluorescence microscopy, as well as caspase 3/7 activity assays. We found that *C. albicans* does not induce apoptosis in C2BBe1 cells, even 24 h p.i. (Fig. 6B to D). In contrast, approximately 40% of IECs exhibited necrotic cell death 24 h p.i. in response to *C. albicans*, as indicated by ethidium homodimer III (EthD-III) staining (Fig. 6C). Therefore, necrotic cell death appears to be the major mechanism supporting *C. albicans* transcellular translocation in our model (Fig. 1, 3, and 6).

Candidalysin is critical for intestinal epithelial damage and fungal translocation. The secretion of the cytolytic peptide toxin candidalysin, encoded by the *ECE1* gene, is known to be critical for oral and vaginal EC damage (35, 52). Given that necrotic cell death appears to be the major mechanism supporting *C. albicans* transcellular translocation, we investigated the role of candidalysin in gut translocation in our *in vitro* model. We found that a *C. albicans* strain lacking *ECE1* was hypodamaging to IECs, was unable to translocate across the gut barrier, and was defective in reducing epithelial integrity (Fig. 3 and 4).

To confirm that candidalysin was required for intestinal cell damage, we infected C2BBe1 cells with either a *C. albicans* mutant that lacked only the candidalysin-encoding region within *ECE1* (*ece1*Δ/Δ+*ECE1*$_{\Delta 184-279}$ mutant) or with synthetic candidalysin toxin (35). Both the *ece1*Δ/Δ mutant and the *ece1*Δ/Δ+*ECE1*$_{\Delta 184-279}$ mutant exhibited normal adhesion, epithelial invasion, and hyphal growth (Fig. 7A, B, and C) but were unable to induce epithelial damage (Fig. 7D), in contrast to the WT strain and a revertant strain expressing one WT copy of *ECE1* (*ece1*Δ/Δ+*ECE1* strain). Interestingly, the addition of synthetic candidalysin to IECs caused only minimal damage (Fig. 7). However, combined administration of candidalysin with the *ece1*Δ/Δ and *ece1*Δ/Δ+*ECE1*$_{\Delta 184-279}$ mutants partially restored the damage capacity of these strains (Fig. 7D). This demonstrates that a combination of hypha formation and candidalysin secretion is required for optimal damage induction of IECs by *C. albicans*.

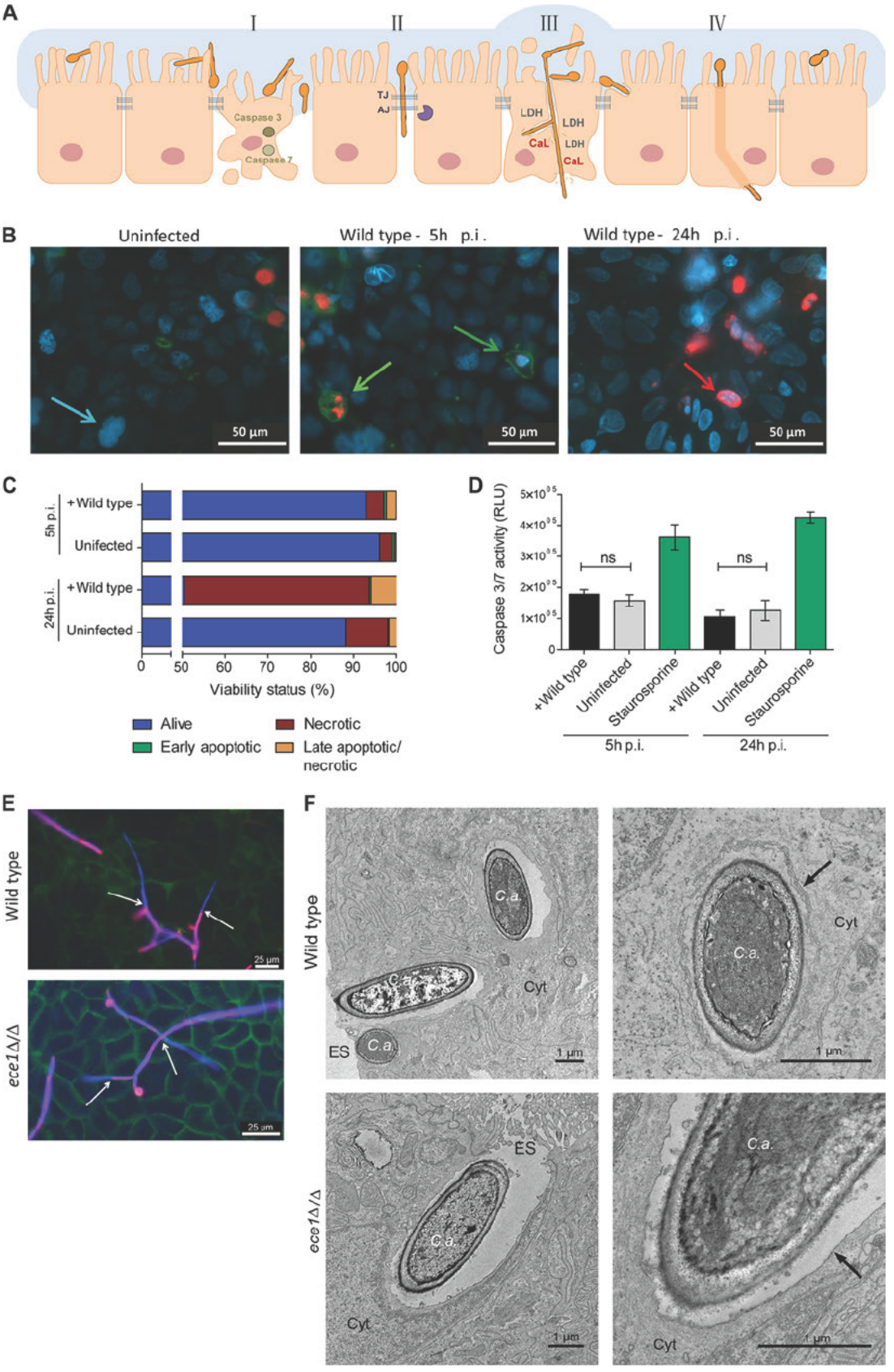

FIG 6 Possible translocation mechanisms of *C. albicans* through IECs. (A) Schematic representation of possible routes of *C. albicans* translocation. Possible routes of *C. albicans* translocation are shown as follows: I, apoptosis; II, paracellular; III, transcellular with

(Continued on next page)

Next, we investigated the influence of candidalysin on intestinal barrier integrity by monitoring TEER and quantifying the diffusion of 4-kDa dextran polymers (Fig. 7E and G). The TEER values of C2BBe1 epithelium infected with WT *C. albicans* or an *ece1*Δ/Δ mutant constantly dropped over a time period of 48 h, but there was retention of TEER for the *ece1*Δ/Δ and *ece1*Δ/Δ+*ECE1*$_{\Delta 184-279}$ mutants between 24 and 32 h p.i. (Fig. 7G). Accordingly, the dextran diffusion assay showed reduced barrier leakage in response to infection with the *ece1*Δ/Δ and *ece1*Δ/Δ+*ECE1*$_{\Delta 184-279}$ mutants (Fig. 7E). In contrast to the damage assay, addition of synthetic candidalysin to C2BBe1 epithelium had no direct (single administration) or indirect (administration together with *ece1*Δ/Δ or *ece1*Δ/Δ+*ECE1*$_{\Delta 184-279}$ mutant) effect on epithelial barrier function (Fig. 7E and G). As a means of comparison, we also administered melittin, a cytolytic peptide toxin in bee venom, as a positive control (53) in the damage and barrier integrity assays. Melittin caused high LDH release (Fig. 7D) and completely abolished epithelial barrier function (Fig. 7E and G).

As an expected consequence of reduced EC damage and reduced loss of integrity, translocation of *ece1*Δ/Δ and *ece1*Δ/Δ+*ECE1*$_{\Delta 184-279}$ mutants was significantly reduced. We observed a trend toward higher translocation of *ece1*Δ/Δ and *ece1*Δ/Δ+*ECE1*$_{\Delta 184-279}$ mutants when candidalysin was added during epithelial infection (Fig. 7F). Of note, while damage was almost abolished in the absence of candidalysin or *ECE1*, translocation of the respective mutants was still possible to a limited extent (approximately 25% of the WT level) (Fig. 4 and 7), emphasizing that translocation can occur without damage and independently of candidalysin. Therefore, we proposed a second route of transcellular translocation, which is not associated with EC damage (Fig. 6A, route IV). In this scenario, hyphae would invade ECs on the apical side and emerge on the basolateral side without causing host membrane damage and without causing release of cellular content (Fig. 6A, route IV). Fluorescence microscopy pictures clearly demonstrate that the hyphae of an *ece1*Δ/Δ mutant can invade and grow through IECs (Fig. 6E) without causing epithelial damage (Fig. 7D). Furthermore, transmission electron microscopy (TEM) pictures of invasive *C. albicans* hyphae show the presence of a host membrane surrounding hyphae in some pictures (Fig. 6F, black arrows), suggesting that transcellular translocation without membrane damage may be possible.

In conclusion, our data show that *C. albicans* is able to translocate through intact intestinal epithelial barriers predominantly via a damage-associated necrotic, but not apoptotic, transcellular route. Disturbance of epithelial integrity, cellular damage, and transcellular translocation requires a combination of fungal properties, including hypha formation and the secretion of candidalysin.

DISCUSSION

The human gastrointestinal tract is colonized by a dense population of microorganisms, including bacteria and fungi. Although the gut epithelial layers and associated immune cells provide a functional barrier between these microbes and the host, microbial translocation is frequent, even in healthy individuals (54). However, in critically ill patients, translocation may lead to life-threatening infections. Several studies

FIG 6 Legend (Continued)
damage; IV, transcellular without damage. TJ, tight junctions; AJ, adherens junctions; CaL, candidalysin. (B) C2BBe1 IECs were infected with WT *C. albicans* SC5314 for 5 h and 24 h and differentially stained. Living cells (Hoechst 33342) (blue), apoptotic cells (FITC-annexin V) (green), necrotic cells (ethidium homodimer III) (red), and late apoptotic/necrotic cells (red/green) are indicated by the color(s) indicated. Colored arrows point to examples of the stained cells. (C) A summary of statistical analysis is presented (mean ± SD; $n = 3$) that quantifies the proportion of live-apoptotic-necrotic staining observed in the images in panel B. (D) Quantification of caspase 3/7 activity in C2BBe1 IECs infected for 5 h and 24 h with *C. albicans* SC5314. Staurosporine was used as a positive control for the induction of apoptosis. Data are presented as means ± SD from three independent experiments. Caspase 3/7 activity is shown in relative light units (RLU). Values that are not significantly different (ns) are indicated. (E) Transcellular growth of WT *C. albicans* (BWP17+Clp30) and *ece1*Δ/Δ mutant hyphae through C2BBe1 IECs. C2BBe1 cells were infected with *C. albicans* and differentially stained at 6 h p.i. Extracellular *C. albicans* (pink), *C. albicans* (blue), and actin (green) are indicated. The white arrows show the point of invasion. (F) TEM images of C2BBe1 IECs infected with WT *C. albicans* (BWP17+Clp30) or *ece1*Δ/Δ mutant. The black arrows point to the host membrane. *C.a.*, *C. albicans*; Cyt, cytoplasm; ES, extracellular space.

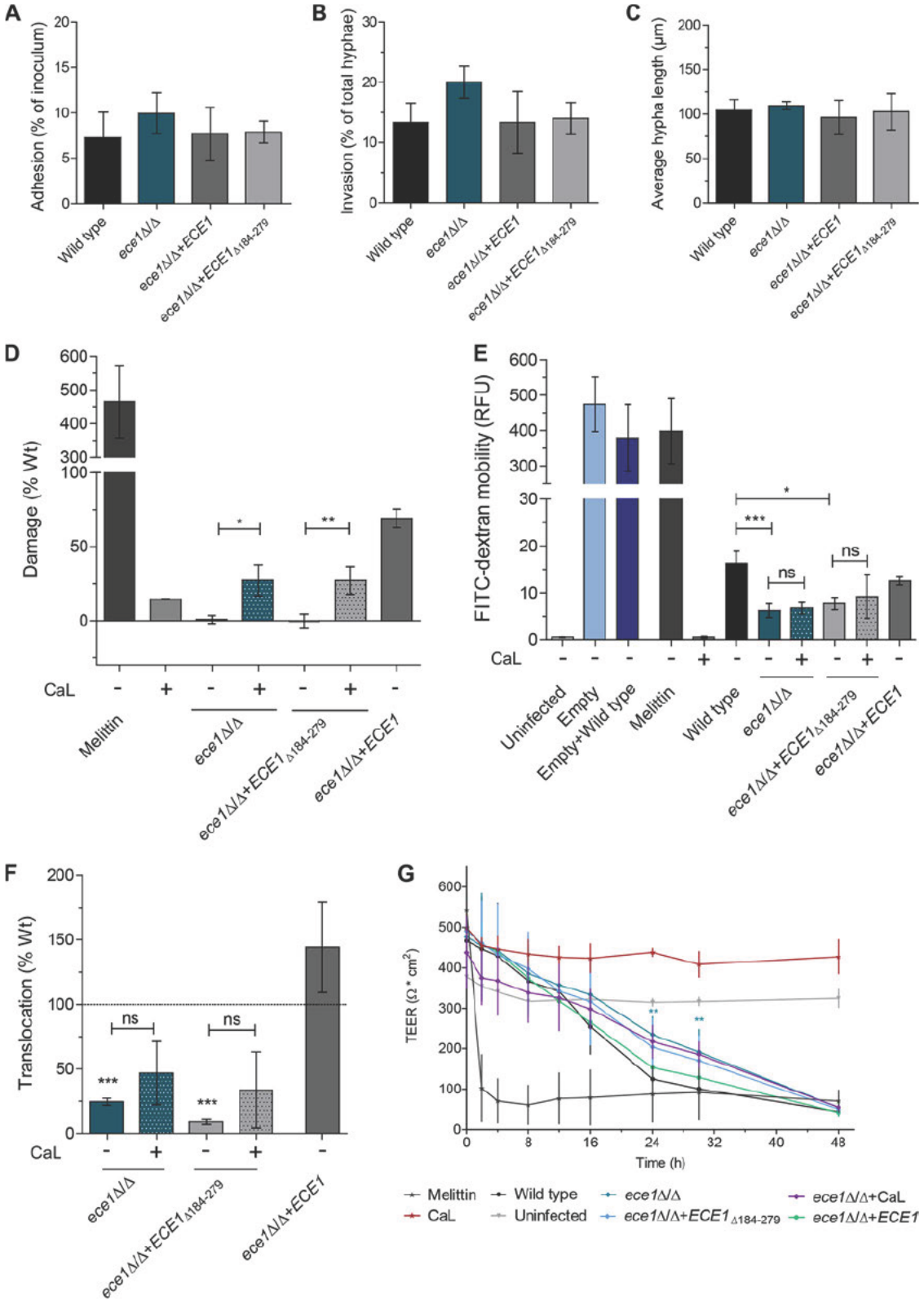

FIG 7 Interaction of *C. albicans ECE1* mutant strains with IECs. (A) Adhesion to C2BBe1 IECs as a percentage of inoculated cells of *C. albicans ECE1* mutant strains. (B) Invasion into C2BBe1 IECs as a percentage of total visible hyphae of *ECE1* mutant strains. (C) C2BBe1 cells were infected with *ECE1* mutant strains, and the mean hyphal length of infecting fungi 6 h p.i. was quantified. (D to G) Quantification of LDH (damage) (D), analysis of epithelial barrier integrity by dextran mobility assay (E), quantification of fungal translocation (F), and epithelial barrier integrity as measured by TEER in response to *C. albicans ECE1* mutant strains (G). In panels D to G, the application of exogenous candidalysin (CaL) toxin (70 μM) alone to C2BBe1 IECs and in combination with infecting *ECE1*

(Continued on next page)

ascribe the major source of systemic candidiasis to the commensal *C. albicans* population of the human intestinal tract (8, 10, 55). However, we know little about how *C. albicans* translocates across intact intestinal epithelial barriers. In this study, we used an *in vitro* model and a reductionist approach to identify the *C. albicans* factors and host mechanisms involved in fungal translocation across the human gut barrier. While previous studies have focused on either *C. albicans* translocation (29, 38), *C. albicans*-dependent epithelial damage (29, 39), or epithelial integrity (39), our study analyzed all three processes over time to identify the fungal factors and host mechanisms associated with *C. albicans* translocation across the intact gut barrier. We demonstrate that *C. albicans* translocation is a dynamic fungus-driven process initiated by invasion (active penetration) and followed by cellular damage and loss of epithelial integrity. Experimental and bioinformatic correlation analyses indicated that epithelial damage and loss of epithelial integrity closely correlated with *C. albicans* translocation. Translocation occurs via a transcellular route, which is associated with fungus-induced necrotic epithelial damage, driven by the cytolytic peptide toxin candidalysin. However, fungal invasion and low-level translocation can also occur in a candidalysin-independent manner.

To identify fungal factors involved in *C. albicans* gut translocation, we screened >2,000 *C. albicans* gene deletion mutants. We identified 172 gene deletion mutants that were hypodamaging, including 38 mutants with no obvious growth or filamentation defects. Of these, eight mutants were selected for further analyses and subsequently found to have defects in adhesion, invasion, and hyphal length or potential defects in transcriptional and cellular regulation or protein trafficking (45–47). The main exception was a *C. albicans ECE1* gene deletion mutant, which had normal hypha formation/length and adhesion to and invasion of IECs but was defective in inducing epithelial damage. Interestingly, *C. albicans ECE1* encodes a cytolytic peptide toxin, candidalysin, which is critical for mucosal infections (35, 36).

Next, using a larger panel of *C. albicans* mutants, we determined that hypha formation was a key fungal attribute that promoted epithelial damage, loss of epithelial integrity, and translocation. However, translocation was not dependent upon hypha formation, as some mutants (e.g., *hgc1*Δ/Δ mutant [56]), which are generally locked in the yeast form or do not maintain hyphae, were still able to translocate across intestinal cells to a limited degree. Notably, though, the *hgc1*Δ/Δ mutant still expressed hypha-associated genes, including *ECE1* (data not shown), again potentially linking candidalysin to gut translocation. These findings may also explain contrasting data from *in vivo* translocation experiments, in which *C. albicans* gut translocation was shown to be both hypha dependent (24) and independent (25). Other proteins that contributed to *C. albicans* damage and translocation included Kex1, a Golgi protease involved in the processing of candidalysin (35, 57), and Als3, a glycosylphosphatidylinositol (GPI)-anchored adhesin and invasin that is the main trigger of induced endocytosis for certain types of epithelial and endothelial cells (33, 58). The *als3*Δ/Δ mutant had strong defects in damage, translocation, and disruption of epithelial integrity. However, since invasion into IECs occurs independently of induced endocytosis (29), we concluded that the observed phenotypes were mostly due to the severely reduced adhesion of this mutant (58) rather than direct action of Als3 on the gut barrier.

Our experimental findings were supported by bioinformatic approaches that also indicated a correlation between damage of IECs and translocation. Interestingly, a cluster of *C. albicans* mutants was identified with reduced epithelial damage but normal fungal translocation (Fig. 4, cluster II), indicating that only a certain level of damage induction is required to achieve efficient translocation. Furthermore, fungal translocation was not observed without reduction in TEER, strongly suggesting that disturbance

FIG 7 Legend (Continued)
mutant strains was assessed. Melittin (70 μM) was used as a positive control for damaging C2BBe1 cells. Data are presented as means ± SD relative to the WT from at least three independent experiments. Statistical significance: *, $P \leq 0.05$; **, $P \leq 0.01$; ***, $P \leq 0.001$; ns, not significant.

of epithelial integrity is a prerequisite for translocation. However, a decrease of epithelial integrity does not necessarily lead to significant fungal translocation (as observed for *pep12*Δ/Δ and orf19.3335Δ/Δ mutants). Hence, TEER loss is necessary but not sufficient to cause fungal translocation. Thus, in agreement with Böhringer et al. (39), we propose that damage and destruction of epithelial integrity can be independent processes and that loss of epithelial integrity may be caused by necrotic cell damage (59) or opening of cell-cell connections (e.g., tight junctions). Epithelial damage and reduction of barrier integrity are likely coupled during necrosis, but loss of epithelial integrity can occur independently of necrosis.

One of the most intriguing findings of the study was the discovery that the hypha-associated peptide toxin candidalysin appears to be a crucial factor in mediating intestinal epithelial damage and fungal translocation. Notably, the combination of exogenous addition of candidalysin to an *ECE1*-deficient strain only partially restored WT damage and translocation levels, and the exogenous addition of candidalysin alone had little effect (Fig. 7). Several studies, including Moyes et al. (35), proposed a membrane-bound "invasion pocket" during hyphal invasion of epithelial cells (29, 60, 61) which was further verified for the C2BBe1 cells in this study (Fig. 6F). This invagination of the epithelial membrane at the site of hyphal invasion results in close contact of the fungus to host membranes and should allow an accumulation of candidalysin that may be required for full damage potential and subsequent translocation. Therefore, the exogenous addition of candidalysin probably does not fully mimic the natural secretion by hyphae within this invasion pocket and thus does not fully restore WT damage levels. It is less likely that the other non-candidalysin Ece1 peptides play a role in this setting, since when adding such peptides together with candidalysin, no increased damage was observed (data not shown); along the same line, adding candidalysin to a candidalysin-deficient strain (*ece1*Δ/Δ+*ECE1*$_{\Delta 184-279}$) also only partially restored WT damage and translocation levels.

However, we noted that while the *ece1*Δ/Δ mutant was unable to damage ECs, it was still able to lower epithelial integrity and translocate across the intestinal barrier to some extent. This suggests that a damage-independent fungal factor(s) can also modulate epithelial integrity. Such a factor(s) probably contributes to the paracellular route of translocation by degrading cell-cell connections such as tight junctions or adherens junctions. Possible candidates contributing to the paracellular route of translocation are the secreted aspartic proteases (SAPs), which may promote degradation of the adherens junction protein E-cadherin (29, 62, 63). However, we found that mutants lacking different *SAP* genes (*sap1-3*Δ/Δ, *sap5*Δ/Δ, *sap4-6*Δ/Δ, and *sap9/10*Δ/Δ mutants) had no translocation defects. This is with the caveat that the *sap1-3*Δ/Δ mutant exhibited reduced translocation through blank transwell inserts (without C2BBe1 cells), and thus, we cannot exclude a minor role for SAPs in the paracellular route of translocation. In summary, our data demonstrate that *C. albicans* translocates across the intestinal epithelial barrier predominantly via the transcellular route, which requires hypha formation, active penetration (not induced endocytosis), candidalysin-induced epithelial damage, and cellular necrosis. However, *C. albicans* can also translocate via the paracellular route in a damage- and candidalysin-independent manner via currently unknown mechanisms.

While our *in vitro* data are likely to be reflective of the *C. albicans* translocation process *in vivo*, host-driven uptake and fungal translocation *in vivo* may also occur via specialized intestinal cells, in particular M cells associated with Peyer's patches, which were not modeled into our assays. M cells are capable of endocytosing *C. albicans* (64) and are targeted by several pathogenic Gram-negative bacteria, including *Shigella*, *Salmonella*, and *Yersinia* spp. (65–67). Nevertheless, our study indicates that efficient *C. albicans* translocation can also occur in the absence of M cells, predominantly via candidalysin-mediated necrotic damage to the intestinal barrier. With this in mind, toxin-induced intestinal barrier dysfunction is also an important factor contributing to the pathogenicity of enteric bacteria. *Clostridium perfringens* produces a number of toxins that impair intestinal barrier function. These toxins include *C. perfringens* δ-toxin,

a β-pore-forming-toxin, which is cytotoxic to Caco-2 cells and functions to reduce epithelial integrity (TEER) and increase permeability without altering tight junctions (68). In contrast, *C. perfringens* enterotoxin (CPE) directly attaches to and disintegrates tight junctions (claudin family), resulting in an increase in paracellular permeability across the epithelial barrier (69). Furthermore, the phospholipase C activity of *C. perfringens* alpha-toxin results in increased gut permeability, most likely due to the redistribution and/or degradation of tight junction proteins (70). Likewise, suilysin, a cholesterol-dependent cytolysin produced by the swine pathogen *Streptococcus suis*, is thought to promote bacterial translocation via epithelial damage induction, although the precise mechanisms are unclear (71). While many other bacteria are capable of translocating across the gut barrier, such as enteropathogenic *Escherichia coli* (EPEC), *Campylobacter jejuni*, and *Salmonella enterica* serotype Typhimurium, the mechanisms by which this occurs may not always be attributed to the function of toxins (72). Irrespective, the majority of enteric bacteria appear to translocate via the paracellular route rather than the transcellular route.

In summary, *C. albicans* translocation predominantly occurs via a transcellular route, associated with candidalysin-induced necrotic epithelial damage. However, invasion and low-level translocation can also occur in a candidalysin-independent manner, most likely via a paracellular route.

MATERIALS AND METHODS

***Candida albicans* strains and growth conditions.** All *C. albicans* strains used in this study are listed in Table S1 in the supplemental material. *C. albicans* strains were routinely grown on YPD broth/agar (1% yeast extract, 2% peptone, 2% D-glucose with or without 1.5% agar) at 30°C. For all experiments, *C. albicans* cells were cultured overnight in YPD broth at 30°C, shaking at 180 rpm. Cells from overnight cultures were collected by centrifugation and washed twice with phosphate-buffered saline (PBS), and the number of cells was adjusted as indicated.

Generation of *C. albicans* mutant strains. Gene deletions were performed as previously described (48). Deletion cassettes were generated by PCR by amplifying pFA-HIS1 and pFA-ARG4-based markers with the respective primers for the gene to be deleted (Data Set S3). *C. albicans* BWP17 was sequentially transformed with the generated deletion cassettes and then transformed with the Clp10 vector (73). All integrations were confirmed by PCR/sequencing. The *sap1-3*Δ/Δ and *sap4-6*Δ/Δ mutants were exceptions; these mutants were created by the Ura-blaster method (74–76).

Culture and maintenance of IEC lines. The intestinal epithelial Caco-2 subclone C2BBe1 (Caco-2 brush border expressing 1; ATCC CRL2102) (37) was routinely cultivated in Dulbecco modified Eagle medium (DMEM) (ThermoFisher Scientific) supplemented with 10% fetal calf serum (FCS) (Bio&Sell) and 10 μg/ml holotransferrin (Calbiochem Merck) in a humidified incubator at 37°C and 5% CO_2. C2BBe1 cells were seeded in collagen I-coated wells (10 μg/ml collagen I for 2 h at room temperature [RT]; ThermoFisher Scientific). Transwell inserts (polycarbonate membrane with 5-μm pores; Corning) and 96-well plates were seeded with 2×10^4 cells/well or insert, and glass coverslips were placed in 24-well plates with 1×10^5 cells/well. C2BBe1 cells were cultured for 14 days for differentiation, with medium exchanged every 3 or 4 days.

The intestinal epithelial cell (IEC) line Caco-2 (ACC 169 from DSMZ) was cultivated in medium supplemented with 10% FCS and 1% NEAA (MEM [minimum essential medium] nonessential amino acids; Biochrom AG), for 2 days. All infections were performed in serum-free DMEM in a humidified incubator at 37°C and 5% CO_2. This cell line was used only for the large-scale mutant screening (see "*C. albicans* large-scale mutant screening" below). For this purpose, Caco-2 cells were seeded in 96-well plates with 2×10^4 cells/well and grown for 2 days to confluence.

***C. albicans* large-scale mutant screening.** *C. albicans* strains were cultivated in YPD broth in 96-well plates and incubated for 24 h at 30°C and 180 rpm. On the next day, a 1:20 subculture was set up in fresh YPD and incubated overnight at 30°C and 180 rpm. The cultures were then diluted 1:10 in PBS. From this dilution, a 1:20 dilution in YPD was used to analyze growth at 30°C (see "Analysis of fungal growth" below), and a 1:20 dilution in serum-free DMEM was used to infect confluent Caco-2 cells. After 24 h of infection, damage was evaluated by quantifying the release of cytoplasmatic lactate dehydrogenase (LDH) [see "Quantification of cytotoxicity (LDH assay)" below]. In the large-scale mutant screening for damage, all values were compared to the values for a uninfected control treated with 0.25% Triton X-100 to obtain full lysis of the Caco-2 cells (full lysis control), and mutant values outside the 2σ range of the WT values were considered significantly different.

Analysis of fungal growth. Fungal growth was analyzed in 96-well plates in YPD broth. The *C. albicans* strains were added at a final density of 4×10^5 cells/well. Growth was monitored by measuring the absorbance at 600 nm every 30 min for 2 days at 30°C in a microplate reader (Tecan).

Quantification of adhesion, invasion, and hypha length. *C. albicans* cells were added to 14-day-old C2BBe1 cells in 24-well plates to a final concentration of 1×10^5 cells/well for adhesion assays and 5×10^4 cells/well for invasion and hypha length assays. Control experiments for hypha length were performed the same way on plastic without C2BBe1 cells.

Adhesion of *C. albicans* to ECs was determined 1 h postinfection (p.i.). Nonattached *C. albicans* cells were removed by washing the cells three times with PBS. Samples were fixed with Histofix (Roth) for 15 min at RT or overnight at 4°C and subsequently rinsed three times with PBS. Adherent fungi were stained with calcofluor white (10 μg/ml in 0.1 M Tris-HCl [pH 9.0]; Sigma-Aldrich) for 20 min at RT in the dark. After the samples were washed three times with water, samples were mounted on glass slides with ProLong mountant (ThermoFisher Scientific) and analyzed by fluorescence microscopy. The number of adherent *C. albicans* cells was determined in about 100 random fields of a defined size (200 by 200 μm). Assuming an even distribution of *Candida* cells, the total number of adherent cells on the entire coverslip was calculated based on the number counted in the defined area. This number was expressed as a percentage of adhered cells versus inoculated *C. albicans* cells (see references 29 and 58 also). Invasion of *C. albicans* into differentiated C2BBe1 cells was analyzed by differential staining performed according to references 58 and 77 with the following minor modifications. Briefly, after 5 h of *C. albicans* infection, C2BBe1 cells were washed three times with PBS and fixed with Histofix. Extracellular, noninvasive fungal components were stained as follows. The cells were incubated with a primary antibody against *C. albicans* (1:2,000 in PBS) (rabbit anti-*Candida* BP1006; Acris Antibodies) for 1 h at 30°C, washed three times with PBS, and incubated with a secondary antibody (1:5,000 in PBS) (goat anti-rabbit antibody labeled with Alexa Fluor 488 [catalog no. A-11008; ThermoFisher Scientific]) for 1 h at 30°C. After the ECs were rinsed three times with PBS, they were permeabilized with 0.5% Triton X-100 for 10 min at RT and washed again three times with PBS. The actin cytoskeleton was stained with phalloidin-Alexa Fluor 594 (1:50 in PBS) (catalog no. A12381; ThermoFisher Scientific) for 1 h at 30°C. After the cells were washed again (three times with PBS), *C. albicans* cells were stained with calcofluor white as described above. After mounting, samples were visualized by fluorescence microscopy. The percentage of invasive *C. albicans* hyphae (only calcofluor white stained) was counted from at least 100 hyphae per strain in at least three independent experiments. The total hypha length was also recorded. For invasion experiments with cytochalasin D (Sigma-Aldrich), 1 μl of cytochalasin D or dimethyl sulfoxide (DMSO) (as solvent control) was added, to a final concentration of 0.5 μM 45 min prior to infection (78).

Quantification of cytotoxicity (LDH assay). Differentiated C2BBe1 cells in 96-well plates were infected for a defined time period with 8×10^4 *C. albicans* cells/well or with candidalysin toxin (sequence, SIIGIIMGILGNIPQVIQIIMSIVKAFKGNK; ProteoGenix/Peptide Protein Research Ltd.) prepared in water and added to the desired final concentration. After coincubation, epithelial damage was quantified by measuring LDH release using a cytotoxicity detection kit (Roche) according to the manufacturer's instructions. LDH isolated from rabbit muscle (Roche) was used to generate a standard curve. The background LDH value of uninfected C2BBe1 cells was subtracted, and the corrected LDH release was expressed as a percentage of the wild-type (WT) values unless otherwise stated. Cytotoxicity analysis was performed in triplicate and finally determined from at least three independent experiments.

***In vitro* translocation model.** Differentiated C2BBe1 cells grown in transwell inserts (Fig. S5) were infected with 1×10^5 *C. albicans* cells per transwell and/or candidalysin toxin for 24 h. Before and after incubation, transepithelial electrical resistance (TEER) values were measured using a volt-ohm meter (WPI). The resistance of a blank insert (≈120 Ω) was subtracted from each value. The absolute TEER loss (in ohms) of the respective WT was set at 100%, and the TEER loss of the mutant strains was expressed as a percentage of the WT value. After 24 h of infection, zymolyase (Amsbio) was added to the basolateral chamber to a final concentration of 20 U/ml and incubated for 2 h at 37°C and 5% CO_2. Afterward, detached *C. albicans* hyphae were collected and plated onto YPD agar. Translocation was measured in triplicate in at least three independent experiments. Each *C. albicans* mutant was additionally tested for general growth, sensitivity against Zymolyase, and translocation independent of C2BBe1 (through a blank insert).

To test for abnormal sensitivity toward zymolyase treatment, *C. albicans* strains were placed in a 96-well plate (1×10^5 cells/well) in serum-free DMEM. After incubation for 3 h at 37°C and 5% CO_2, zymolyase was added to a final concentration of 20 U/ml. Cells were incubated for 2 h, diluted in PBS, and plated onto YPD agar. Colonies were counted after 2 days and compared to the respective WT.

The translocation rate of *C. albicans* strains through blank, collagen I-coated transwell inserts was measured as indicated above. However, *C. albicans* strains were incubated in DMEM at 37°C and 5% CO_2 for 3 h before addition to the inserts to induce filamentation and to reduce unspecific translocation of yeast cells. Blank translocation was used to correct the translocation rate through C2BBe1 cells. For each mutant, the efficiency of fungal translocation was calculated for each biological replicate. The percent translocation (TL) compared to the wild type (WT) was calculated as follows:

$$\%\,\mathrm{TL} = \left(\frac{\text{TL of mutant}}{\text{TL of WT}}\right)\left(\frac{\overline{\text{blank TL of WT}}}{\overline{\text{blank TL of mutant}}}\right) \times 100$$

Analysis of epithelial barrier integrity by dextran diffusion assay. Dextran diffusion assays were performed by the method of Elamin et al. (79) with the following modifications. Briefly, fluorescein isothiocyanate (FITC)-labeled 4-kDa dextran beads (Sigma-Aldrich) were used to analyze the permeability of differentiated C2BBe1 monolayers infected with 1×10^5 *C. albicans* cells/transwell insert and/or candidalysin for 24 h in serum- and pH indicator-free DMEM. After incubation, 30 μl of dextran beads (50 mg/ml in PBS) was added to the apical compartment and incubated for 3 h at 37°C and 5% CO_2. Fluorescence (excitation wavelength of 490 nm and emission wavelength of 520 nm) of diffused dextran beads was measured in the basolateral transwell compartment. The background fluorescence of DMEM was subtracted from each value. Analyses were performed in duplicate and determined from at least three independent experiments.

Analysis of apoptosis and necrosis. Apoptosis and necrosis of differentiated C2BBe1 cells after infection with *C. albicans* were quantified using the apoptotic/necrotic/healthy cell detection kit (PromoKine) according to the manufacturer's instructions. Differentiated C2BBe1 cells were infected with 1×10^5 *C. albicans* cells/well for 5 h or 5×10^4 cells/well for 24 h, then washed, and incubated for 15 min in the dark with FITC-annexin V, ethidium homodimer II, and Hoechst 33342. After the infected cells were washed, they were examined by fluorescence microscopy (Zeiss Axio Observer). Uninfected, differentiated C2BBe1 cells were used as a negative control. Treatment with 40% ethanol for 1 min was used as a positive control for necrosis, and treatment with 2 μM staurosporine was used as a positive control for apoptosis.

The activity of caspase 3 and 7 was quantified using a Caspase-Glo 3/7 assay (Promega) according to the manufacturer's instructions. Differentiated C2BBe1 cells in 96-well plates were infected with 2×10^4 *C. albicans* cells/well for 5 h or 24 h. The volume of medium in each well was adjusted to 50 μl, and 50 μl of Caspase-Glo 3/7 reagent was added to each well. After the addition of Caspase-Glo 3/7 reagent, luminescence measurements were taken every 10 min for 2 h at RT in the dark using a microplate reader. Each measurement was performed in duplicate, and the mean value was calculated from three independent experiments.

Cluster analysis and correlation coefficient calculation. Cluster analysis enabled *C. albicans* mutants to be assigned into groups with similar behavior regarding the three measurements "epithelial damage," "epithelial integrity" and "fungal translocation," as described by the values LDH, TEER and translocation. Clusters were identified in Python using the scikit-learn library (81) applying the density-based spatial clustering of applications with noise (DBSCAN) algorithm (49). A cluster was detected if (i) it contained at least three members and (ii) the points were closer than $\varepsilon = 35$ percentage points (pp) to at least one other member. DBSCAN automatically finds the number of clusters, and all points that are not considered part of any cluster were left unassigned.

For correlation coefficient calculation, two of the three parameters epithelial damage (LDH)/epithelial integrity (TEER)/fungal translocation were plotted against each other, using the median response of all mutants as a percentage of the WT. For epithelial integrity, a TEER loss of 100% reflects the drop in TEER caused by the WT, while the 100% LDH and translocation values are the epithelial damage and translocation of the WT. Both the Pearson and Spearman correlation coefficients between measurements were calculated. To visualize overall trends, the locally weighted scatterplot smoothing (LOWESS) line was used (51, 80). To evaluate the linearity, or lack thereof, we fitted a first-order polynomial and an exponential function of the formula $y = Ae^{-\alpha x} + B$, representing linear and nonlinear relationships, respectively. We evaluated whether the exponential fit added any information about the pairwise relationship by calculating the Bayesian information criterion (BIC) for each fit. The BIC is defined as follows: $\mathrm{BIC} = (n)\left(\log\frac{\mathrm{RSS}}{n}\right) + k(\log n)$ where n is the number of fitted points, k is the number of parameters in the model, and RSS is the sum of squared residuals (50).

For the cluster analysis and correlation coefficient calculation, the median values of the data were used to reduce the effect of outliers.

Transmission electron microscopy of *C. albicans*-infected C2BBe1 cells. Differentiated C2BBe1 cells were infected with 2×10^5 *C. albicans* cells/transwell. After coincubation for 24 h, cells were fixed with Karnovsky fixative (3% paraformaldehyde, 3.6% glutaraldehyde, pH 7.2) for 24 h at 4°C and postfixed with osmium solution (1% OsO_4 [Roth] and 1.5% potassium ferrocyanide [Morphisto]) for 2 h at 4°C. Samples were rinsed with distilled water, block stained with uranyl acetate (2% in double-distilled water [ddH_2O]), dehydrated in alcohol (stepwise 50 to 100%), and embedded in glycide ether (Serva) by polymerizing for 48 h at 60°C. Semithin sections of 1 μm were cut on an Ultracut Nova instrument (Leica) with a diamond knife and stained with toluidine blue stain (Morphisto) at 80°C. Regions of interest were ultrathin sectioned at 30 nm, mounted on copper grids, and analyzed using a Zeiss LIBRA 120 transmission electron microscope (Carl Zeiss, Inc.) operating at 120 kV.

Statistical analysis. All experiments were conducted, including technical duplicates or triplicates (from which the mean value was calculated) on at least three independent occasions (biological replicates). Diagrams show the mean of the biological replicates with standard deviation (SD). Statistics relative to the WT control were performed on log-transformed values by means of a one-way analysis of variance (ANOVA) test with a follow-up test for multiple comparisons (Dunnett's correction). When comparisons were made between selected data sets, a Bonferroni's correction was used instead. TEER time curves were statistically tested using two-way ANOVA.

SUPPLEMENTAL MATERIAL

Supplemental material for this article may be found at https://doi.org/10.1128/mBio.00915-18.

FIG S1, TIF file, 3.2 MB.
FIG S2, TIF file, 3.5 MB.
FIG S3, TIF file, 23.5 MB.
FIG S4, TIF file, 8.9 MB.
FIG S5, TIF file, 9.2 MB.
TABLE S1, DOCX file, 0.05 MB.
TABLE S2, DOCX file, 0.1 MB.
DATA SET S1, XLSX file, 0.1 MB.

DATA SET S2, XLSX file, 0.04 MB.
DATA SET S3, XLSX file, 0.01 MB.

ACKNOWLEDGMENTS

This work was supported in parts by the Deutsche Forschungsgemeinschaft (DFG) within the Collaborative Research Centre (CRC)/Transregio 124 Fungi Net (project C1 [B. Hube], project C2 [J. Morschhäuser], project C5 [I. D. Jacobsen], and project B4 [M. T. Figge]) and the Research Fellowship GZ:HE7565/1-1 to B. Hebecker. This work was further supported by grants from the Medical Research Council (MR/M011372/1), Biotechnology & Biological Sciences Research Council (BB/N014677/1), FP7-PEOPLE-2013-Initial Training Network (606786), National Institutes of Health (R37-DE022550), King's Health Partners Challenge Fund (R170501), the Rosetrees Trust (M680), and the NIH Research at Guys and St. Thomas's NHS Foundation Trust and the King's College London Biomedical Research Centre (IS-BRC-1215-20006) to J. R. Naglik. S. Allert, S. Rudolphi, and T. M. Förster are members of the Jena School for Microbial Communication (JSMC).

The hgc1Δ/Δ and als3Δ/Δ strains were gifts from Y. Wang and A. P. Mitchell. We thank M. Böhringer (ZIK Septomics, Jena) for help and advice during establishment of the transwell system.

The funders had no role in study design, data collection and interpretation, or the decision to submit the work for publication.

REFERENCES

1. Ghannoum MA, Jurevic RJ, Mukherjee PK, Cui F, Sikaroodi M, Naqvi A, Gillevet PM. 2010. Characterization of the oral fungal microbiome (mycobiome) in healthy individuals. PLoS Pathog 6:e1000713. https://doi.org/10.1371/journal.ppat.1000713.
2. Drell T, Lillsaar T, Tummeleht L, Simm J, Aaspõllu A, Väin E, Saarma I, Salumets A, Donders GG, Metsis M. 2013. Characterization of the vaginal micro- and mycobiome in asymptomatic reproductive-age Estonian women. PLoS One 8:e54379. https://doi.org/10.1371/journal.pone.0054379.
3. Williams DW, Jordan RP, Wei XQ, Alves CT, Wise MP, Wilson MJ, Lewis MA. 2013. Interactions of Candida albicans with host epithelial surfaces. J Oral Microbiol 5:22434. https://doi.org/10.3402/jom.v5i0.22434.
4. Brown GD, Denning DW, Gow NA, Levitz SM, Netea MG, White TC. 2012. Hidden killers: human fungal infections. Sci Transl Med 4:165rv13. https://doi.org/10.1126/scitranslmed.3004404.
5. Krause W, Matheis H, Wulf K. 1969. Fungaemia and funguria after oral administration of *Candida albicans*. Lancet i:598–599.
6. Reagan DR, Pfaller MA, Hollis RJ, Wenzel RP. 1990. Characterization of the sequence of colonization and nosocomial candidemia using DNA fingerprinting and a DNA probe. J Clin Microbiol 28:2733–2738.
7. Voss A, Hollis RJ, Pfaller MA, Wenzel RP, Doebbeling BN. 1994. Investigation of the sequence of colonization and candidemia in nonneutropenic patients. J Clin Microbiol 32:975–980.
8. Nucci M, Anaissie E. 2001. Revisiting the source of candidemia: skin or gut? Clin Infect Dis 33:1959–1967. https://doi.org/10.1086/323759.
9. Bougnoux ME, Diogo D, François N, Sendid B, Veirmeire S, Colombel JF, Bouchier C, Van Kruiningen H, d'Enfert C, Poulain D. 2006. Multilocus sequence typing reveals intrafamilial transmission and microevolutions of *Candida albicans* isolates from the human digestive tract. J Clin Microbiol 44:1810–1820. https://doi.org/10.1128/JCM.44.5.1810-1820.2006.
10. Miranda LN, van der Heijden IM, Costa SF, Sousa AP, Sienra RA, Gobara S, Santos CR, Lobo RD, Pessoa VP, Jr, Levin AS. 2009. *Candida* colonisation as a source for candidaemia. J Hosp Infect 72:9–16. https://doi.org/10.1016/j.jhin.2009.02.009.
11. Gouba N, Drancourt M. 2015. Digestive tract mycobiota: a source of infection. Med Mal Infect 45:9–16. https://doi.org/10.1016/j.medmal.2015.01.007.
12. Guttman JA, Finlay BB. 2009. Tight junctions as targets of infectious agents. Biochim Biophys Acta 1788:832–841. https://doi.org/10.1016/j.bbamem.2008.10.028.
13. Kavanaugh NL, Zhang AQ, Nobile CJ, Johnson AD, Ribbeck K. 2014. Mucins suppress virulence traits of *Candida albicans*. mBio 5:e01911. https://doi.org/10.1128/mBio.01911-14.
14. Neville BA, d'Enfert C, Bougnoux ME. 2015. Candida albicans commensalism in the gastrointestinal tract. FEMS Yeast Res 15:fov081. https://doi.org/10.1093/femsyr/fov081.
15. Swidergall M, Ernst JF. 2014. Interplay between *Candida albicans* and the antimicrobial peptide armory. Eukaryot Cell 13:950–957. https://doi.org/10.1128/EC.00093-14.
16. Conti HR, Gaffen SL. 2015. IL-17-mediated immunity to the opportunistic fungal pathogen Candida albicans. J Immunol 195:780–788. https://doi.org/10.4049/jimmunol.1500909.
17. Pfaller MA, Diekema DJ. 2007. Epidemiology of invasive candidiasis: a persistent public health problem. Clin Microbiol Rev 20:133–163. https://doi.org/10.1128/CMR.00029-06.
18. Pasqualotto AC, Nedel WL, Machado TS, Severo LC. 2006. Risk factors and outcome for nosocomial breakthrough candidaemia. J Infect 52:216–222. https://doi.org/10.1016/j.jinf.2005.04.020.
19. Vincent JL, Norrenberg M. 2009. Intensive care unit-acquired weakness: framing the topic. Crit Care Med 37(10 Suppl):S296–S298. https://doi.org/10.1097/CCM.0b013e3181b6f1e1.
20. Zaoutis TE, Argon J, Chu J, Berlin JA, Walsh TJ, Feudtner C. 2005. The epidemiology and attributable outcomes of candidemia in adults and children hospitalized in the United States: a propensity analysis. Clin Infect Dis 41:1232–1239. https://doi.org/10.1086/496922.
21. Wisplinghoff H, Ebbers J, Geurtz L, Stefanik D, Major Y, Edmond MB, Wenzel RP, Seifert H. 2014. Nosocomial bloodstream infections due to *Candida* spp. in the USA: species distribution, clinical features and antifungal susceptibilities. Int J Antimicrob Agents 43:78–81. https://doi.org/10.1016/j.ijantimicag.2013.09.005.
22. Mavor AL, Thewes S, Hube B. 2005. Systemic fungal infections caused by *Candida* species: epidemiology, infection process and virulence attributes. Curr Drug Targets 6:863–874. https://doi.org/10.2174/138945005774912735.
23. Vautier S, Drummond RA, Redelinghuys P, Murray GI, MacCallum DM, Brown GD. 2012. Dectin-1 is not required for controlling *Candida albicans* colonization of the gastrointestinal tract. Infect Immun 80:4216–4222. https://doi.org/10.1128/IAI.00559-12.
24. Koh AY, Köhler JR, Coggshall KT, Van Rooijen N, Pier GB. 2008. Mucosal damage and neutropenia are required for Candida albicans dissemination. PLoS Pathog 4:e35. https://doi.org/10.1371/journal.ppat.0040035.
25. Vautier S, Drummond RA, Chen K, Murray GI, Kadosh D, Brown AJ, Gow NA, MacCallum DM, Kolls JK, Brown GD. 2015. *Candida albicans* coloni-

zation and dissemination from the murine gastrointestinal tract: the influence of morphology and Th17 immunity. Cell Microbiol 17:445–450. https://doi.org/10.1111/cmi.12388.
26. Koh AY. 2013. Murine models of *Candida* gastrointestinal colonization and dissemination. Eukaryot Cell 12:1416–1422. https://doi.org/10.1128/EC.00196-13.
27. Bendel CM, Wiesner SM, Garni RM, Cebelinski E, Wells CL. 2002. Cecal colonization and systemic spread of *Candida albicans* in mice treated with antibiotics and dexamethasone. Pediatr Res 51:290–295. https://doi.org/10.1203/00006450-200203000-00005.
28. Naglik JR, Moyes DL, Wächtler B, Hube B. 2011. *Candida albicans* interactions with epithelial cells and mucosal immunity. Microbes Infect 13:963–976. https://doi.org/10.1016/j.micinf.2011.06.009.
29. Dalle F, Wächtler B, L'Ollivier C, Holland G, Bannert N, Wilson D, Labruère C, Bonnin A, Hube B. 2010. Cellular interactions of *Candida albicans* with human oral epithelial cells and enterocytes. Cell Microbiol 12:248–271. https://doi.org/10.1111/j.1462-5822.2009.01394.x.
30. Gow NA, Hube B. 2012. Importance of the Candida albicans cell wall during commensalism and infection. Curr Opin Microbiol 15:406–412. https://doi.org/10.1016/j.mib.2012.04.005.
31. Jacobsen ID, Hube B. 2017. *Candida albicans* morphology: still in focus. Expert Rev Anti Infect Ther 15:327–330. https://doi.org/10.1080/14787210.2017.1290524.
32. Cota E, Hoyer LL. 2015. The *Candida albicans* agglutinin-like sequence family of adhesins: functional insights gained from structural analysis. Future Microbiol 10:1635–1548. https://doi.org/10.2217/fmb.15.79.
33. Phan QT, Myers CL, Fu Y, Sheppard DC, Yeaman MR, Welch WH, Ibrahim AS, Edwards JE, Jr, Filler SG. 2007. Als3 is a Candida albicans invasin that binds to cadherins and induces endocytosis by host cells. PLoS Biol 5:e64. https://doi.org/10.1371/journal.pbio.0050064.
34. Almeida RS, Brunke S, Albrecht A, Thewes S, Laue M, Edwards JE, Filler SG, Hube B. 2008. The hyphal-associated adhesin and invasin Als3 of Candida albicans mediates iron acquisition from host ferritin. PLoS Pathog 4:e1000217. https://doi.org/10.1371/journal.ppat.1000217.
35. Moyes DL, Wilson D, Richardson JP, Mogavero S, Tang SX, Wernecke J, Höfs S, Gratacap RL, Robbins J, Runglall M, Murciano C, Blagojevic M, Thavaraj S, Förster TM, Hebecker B, Kasper L, Vizcay G, Iancu SI, Kichik N, Häder A, Kurzai O, Luo T, Krüger T, Kniemeyer O, Cota E, Bader O, Wheeler RT, Gutsmann T, Hube B, Naglik JR. 2016. Candidalysin is a fungal peptide toxin critical for mucosal infection. Nature 532:64–68. https://doi.org/10.1038/nature17625.
36. Wilson D, Naglik JR, Hube B. 2016. The missing link between *Candida albicans* hyphal morphogenesis and host cell damage. PLoS Pathog 12:e1005867. https://doi.org/10.1371/journal.ppat.1005867.
37. Peterson MD, Mooseker MS. 1992. Characterization of the enterocyte-like brush border cytoskeleton of the C2BBe clones of the human intestinal cell line, Caco-2. J Cell Sci 102:581–600.
38. Weide MR, Ernst JF. 1999. Caco-2 monolayer as a model for transepithelial migration of the fungal pathogen Candida albicans. Mycoses 42(Suppl 2):61–67. https://doi.org/10.1111/j.1439-0507.1999.tb00015.x.
39. Böhringer M, Pohlers S, Schulze S, Albrecht-Eckardt D, Piegsa J, Weber M, Martin R, Hünniger K, Linde J, Guthke R, Kurzai O. 2016. *Candida albicans* infection leads to barrier breakdown and a MAPK/NF-kappaB mediated stress response in the intestinal epithelial cell line C2BBe1. Cell Microbiol 18:889–904. https://doi.org/10.1111/cmi.12566.
40. Goyer M, Loiselet A, Bon F, L'Ollivier C, Laue M, Holland G, Bonnin A, Dalle F. 2016. Intestinal cell tight junctions limit invasion of *Candida albicans* through active penetration and endocytosis in the early stages of the interaction of the fungus with the intestinal barrier. PLoS One 11:e0149159. https://doi.org/10.1371/journal.pone.0149159.
41. Noble SM, French S, Kohn LA, Chen V, Johnson AD. 2010. Systematic screens of a Candida albicans homozygous deletion library decouple morphogenetic switching and pathogenicity. Nat Genet 42:590–598. https://doi.org/10.1038/ng.605.
42. Nobile CJ, Mitchell AP. 2009. Large-scale gene disruption using the UAU1 cassette. Methods Mol Biol 499:175–194. https://doi.org/10.1007/978-1-60327-151-6_17.
43. Homann OR, Dea J, Noble SM, Johnson AD. 2009. A phenotypic profile of the Candida albicans regulatory network. PLoS Genet 5:e1000783. https://doi.org/10.1371/journal.pgen.1000783.
44. Skrzypek MS, Binkley J, Binkley G, Miyasato SR, Simison M, Sherlock G. 2017. The Candida Genome Database (CGD): incorporation of Assembly 22, systematic identifiers and visualization of high throughput sequencing data. Nucleic Acids Res 45:D592–D596. https://doi.org/10.1093/nar/gkw924.
45. Fu Y, Filler SG, Spellberg BJ, Fonzi W, Ibrahim AS, Kanbe T, Ghannoum MA, Edwards JE, Jr. 1998. Cloning and characterization of *CAD1/AAF1*, a gene from *Candida albicans* that induces adherence to endothelial cells after expression in *Saccharomyces cerevisiae*. Infect Immun 66:2078–2084.
46. Rieg G, Fu Y, Ibrahim AS, Zhou X, Filler SG, Edwards JE, Jr. 1999. Unanticipated heterogeneity in growth rate and virulence among *Candida albicans AAF1* null mutants. Infect Immun 67:3193–3198.
47. Palanisamy SK, Ramirez MA, Lorenz M, Lee SA. 2010. *Candida albicans* PEP12 is required for biofilm integrity and in vivo virulence. Eukaryot Cell 9:266–277. https://doi.org/10.1128/EC.00295-09.
48. Wilson RB, Davis D, Mitchell AP. 1999. Rapid hypothesis testing with *Candida albicans* through gene disruption with short homology regions. J Bacteriol 181:1868–1874.
49. Ester M, Kriegel H-P, Sander J, Xu X. 1996. A density-based algorithm for discovering clusters in large spatial databases with noise, p 226–231. *In* Simoudis E, Han J, Fayyad U (ed), Proceedings of the Second International Conference on Knowledge Discovery and Data Mining. Association for the Advancement of Artificial Intelligence, Palo Alto, CA.
50. Hastie T, Tibshirani R, Friedman J. 2009. The elements of statistical learning. Data mining, inference, and prediction, 2nd ed. Springer, Berlin, Germany.
51. Cleveland WS. 1979. Robust locally weighted regression and smoothing scatterplots. J Am Stat Assoc 74:829–836. https://doi.org/10.1080/01621459.1979.10481038.
52. Richardson JP, Willems HME, Moyes DL, Shoaie S, Barker KS, Tan SL, Palmer GE, Hube B, Naglik JR, Peters BM. 2017. Candidalysin drives epithelial signaling, neutrophil recruitment, and immunopathology at the vaginal mucosa. Infect Immun 86:e00645-17. https://doi.org/10.1128/IAI.00645-17.
53. Maher S, Feighery L, Brayden DJ, McClean S. 2007. Melittin as an epithelial permeability enhancer I: investigation of its mechanism of action in Caco-2 monolayers. Pharm Res 24:1336–1345. https://doi.org/10.1007/s11095-007-9288-2.
54. Wiest R, Rath HC. 2003. Gastrointestinal disorders of the critically ill. Bacterial translocation in the gut. Best Pract Res Clin Gastroenterol 17:397–425. https://doi.org/10.1016/S1521-6918(03)00024-6.
55. Eggimann P, Garbino J, Pittet D. 2003. Epidemiology of *Candida* species infections in critically ill non-immunosuppressed patients. Lancet Infect Dis 3:685–702. https://doi.org/10.1016/S1473-3099(03)00801-6.
56. Zheng X, Wang Y, Wang Y. 2004. Hgc1, a novel hypha-specific G1 cyclin-related protein regulates *Candida albicans* hyphal morphogenesis. EMBO J 23:1845–1856. https://doi.org/10.1038/sj.emboj.7600195.
57. Richardson JP, Mogavero S, Moyes DL, Blagojevic M, Krüger T, Verma AH, Coleman BM, De La Cruz Diaz J, Schulz D, Ponde NO, Carrano G, Kniemeyer O, Wilson D, Bader O, Enoiu SI, Ho J, Kichik N, Gaffen SL, Hube B, Naglik JR. 2018. Processing of Candida albicans Ece1p is critical for candidalysin maturation and fungal virulence. mBio 9:e02178-17. https://doi.org/10.1128/mBio.02178-17.
58. Wächtler B, Wilson D, Haedicke K, Dalle F, Hube B. 2011. From attachment to damage: defined genes of *Candida albicans* mediate adhesion, invasion and damage during interaction with oral epithelial cells. PLoS One 6:e17046. https://doi.org/10.1371/journal.pone.0017046.
59. Konsoula R, Barile FA. 2005. Correlation of *in vitro* cytotoxicity with paracellular permeability in Caco-2 cells. Toxicol In Vitro 19:675–684. https://doi.org/10.1016/j.tiv.2005.03.006.
60. Alexander JW, Boyce ST, Babcock GF, Gianotti L, Peck MD, Dunn DL, Pyles T, Childress CP, Ash SK. 1990. The process of microbial translocation. Ann Surg 212:496–512.
61. Zakikhany K, Naglik JR, Schmidt-Westhausen A, Holland G, Schaller M, Hube B. 2007. In vivo transcript profiling of Candida albicans identifies a gene essential for interepithelial dissemination. Cell Microbiol 9:2938–2954. https://doi.org/10.1111/j.1462-5822.2007.01009.x.
62. Villar CC, Kashleva H, Nobile CJ, Mitchell AP, Dongari-Bagtzoglou A. 2007. Mucosal tissue invasion by *Candida albicans* is associated with E-cadherin degradation, mediated by transcription factor Rim101p and protease Sap5p. Infect Immun 75:2126–2135. https://doi.org/10.1128/IAI.00054-07.
63. Frank CF, Hostetter MK. 2007. Cleavage of E-cadherin: a mechanism for disruption of the intestinal epithelial barrier by *Candida albicans*. Transl Res 149:211–222. https://doi.org/10.1016/j.trsl.2006.11.006.
64. Albac S, Schmitz A, Lopez-Alayon C, d'Enfert C, Sautour M, Ducreux A,

Labruère-Chazal C, Laue M, Holland G, Bonnin A, Dalle F. 2016. Candida albicans is able to use M cells as a portal of entry across the intestinal barrier in vitro. Cell Microbiol 18:195–210. https://doi.org/10.1111/cmi.12495.

65. Sansonetti PJ, Arondel J, Cantey JR, Prévost MC, Huerre M. 1996. Infection of rabbit Peyer's patches by *Shigella flexneri*: effect of adhesive or invasive bacterial phenotypes on follicle-associated epithelium. Infect Immun 64:2752–2764.
66. Lim JS, Na HS, Lee HC, Choy HE, Park SC, Han JM, Cho KA. 2009. Caveolae-mediated entry of *Salmonella typhimurium* in a human M-cell model. Biochem Biophys Res Commun 390:1322–1327. https://doi.org/10.1016/j.bbrc.2009.10.145.
67. Clark MA, Hirst BH, Jepson MA. 1998. M-cell surface beta1 integrin expression and invasin-mediated targeting of *Yersinia pseudotuberculosis* to mouse Peyer's patch M cells. Infect Immun 66:1237–1243.
68. Seike S, Takehara M, Takagishi T, Miyamoto K, Kobayashi K, Nagahama M. 2018. Delta-toxin from *Clostridium perfringens* perturbs intestinal epithelial barrier function in Caco-2 cell monolayers. Biochim Biophys Acta 1860:428–433. https://doi.org/10.1016/j.bbamem.2017.10.003.
69. Saitoh Y, Suzuki H, Tani K, Nishikawa K, Irie K, Ogura Y, Tamura A, Tsukita S, Fujiyoshi Y. 2015. Tight junctions. Structural insight into tight junction disassembly by *Clostridium perfringens* enterotoxin. Science 347:775–778. https://doi.org/10.1126/science.1261833.
70. Otamiri T. 1989. Phospholipase C-mediated intestinal mucosal damage is ameliorated by quinacrine. Food Chem Toxicol 27:399–402. https://doi.org/10.1016/0278-6915(89)90146-4.
71. Ferrando ML, Schultsz C. 2016. A hypothetical model of host-pathogen interaction of *Streptococcus suis* in the gastro-intestinal tract. Gut Microbes 7:154–162. https://doi.org/10.1080/19490976.2016.1144008.
72. Awad WA, Hess C, Hess M. 2017. Enteric pathogens and their toxin-induced disruption of the intestinal barrier through alteration of tight junctions in chickens. Toxins 9:E60. https://doi.org/10.3390/toxins9020060.
73. Murad AM, Lee PR, Broadbent ID, Barelle CJ, Brown AJ. 2000. Clp10, an efficient and convenient integrating vector for Candida albicans. Yeast 16:325–327. https://doi.org/10.1002/1097-0061(20000315)16:4<325::AID-YEA538>3.0.CO;2-%23.
74. Fonzi WA, Irwin MY. 1993. Isogenic strain construction and gene mapping in *Candida albicans*. Genetics 134:717–728.
75. Hube B, Sanglard D, Odds FC, Hess D, Monod M, Schäfer W, Brown AJ, Gow NA. 1997. Disruption of each of the secreted aspartyl proteinase genes *SAP1*, *SAP2*, and *SAP3* of *Candida albicans* attenuates virulence. Infect Immun 65:3529–3538.
76. Sanglard D, Hube B, Monod M, Odds FC, Gow NA. 1997. A triple deletion of the secreted aspartyl proteinase genes *SAP4*, *SAP5*, and *SAP6* of *Candida albicans* causes attenuated virulence. Infect Immun 65:3539–3546.
77. Park H, Myers CL, Sheppard DC, Phan QT, Sanchez AA, Edwards JE, Filler SG. 2005. Role of the fungal Ras-protein kinase A pathway in governing epithelial cell interactions during oropharyngeal candidiasis. Cell Microbiol 7:499–510. https://doi.org/10.1111/j.1462-5822.2004.00476.x.
78. Wächtler B, Citiulo F, Jablonowski N, Förster S, Dalle F, Schaller M, Wilson D, Hube B. 2012. Candida albicans-epithelial interactions: dissecting the roles of active penetration, induced endocytosis and host factors on the infection process. PLoS One 7:e36952. https://doi.org/10.1371/journal.pone.0036952.
79. Elamin E, Masclee A, Troost F, Dekker J, Jonkers D. 2014. Activation of the epithelial-to-mesenchymal transition factor Snail mediates acetaldehyde-induced intestinal epithelial barrier disruption. Alcohol Clin Exp Res 38:344–353. https://doi.org/10.1111/acer.12234.
80. Cleveland WS, Devlin SJ. 1988. Locally weighted regression: an approach to regression analysis by local fitting. J Am Stat Assoc 83:596–610. https://doi.org/10.1080/01621459.1988.10478639.
81. Pedregosa F, Varoquaux G, Gramfort A, Michel V, Thirion B, Grisel O, Blondel M, Prettenhofer P, Weiss R, Dubourg V, Vanderplas J, Passos A, Cournapeau D, Brucher M, Perrot M, Duchesnay E. 2011. Scikit-learn: machine learning in Python. J Machine Learning Research 12:2825–2830. arXiv:1201.0490.